

Spatial Priming for Detecting Human-Object Interactions

Ankan Bansal*, Sai Saketh Rambhatla*, Abhinav Shrivastava, and Rama Chellappa

University of Maryland, College Park, MD, USA
{[@umiacs.umd.edu](mailto:ankan,rssaketh,abhinav,rama)}

Abstract. The relative spatial layout of a human and an object is an important cue for determining how they interact. However, until now, spatial layout has been used just as side-information for detecting human-object interactions (HOIs). In this paper, we present a method for exploiting this spatial layout information for detecting HOIs in images. The proposed method consists of a layout module which primes a visual module to predict the type of interaction between a human and an object. The visual and layout modules share information through lateral connections at several stages. The model uses predictions from the layout module as a prior to the visual module and the prediction from the visual module is given as the final output. It also incorporates semantic information about the object using word2vec vectors. The proposed model reaches an mAP of 24.79% for HICO-Det dataset which is about 2.8% absolute points higher than the current state-of-the-art.

1 Introduction

Detecting human-object interactions (HOIs) involves localizing the interacting humans and objects and correctly predicting the type of interaction (predicate) between them. Humans can guess the type of interaction with just a quick glance at an image by considering the relative locations of the human and the object. For example, in figure 1, the person on the left is very likely to be **sitting** on Chair-1 and **not interacting** with Chair-2. Similarly, the person in the middle is probably **dragging** the suitcase and the human on the right is **standing** on the snowboard and possibly **riding** it. This ability to use spatial relationships helps us in making guesses and eliminating improbable predictions. With additional visual information, we can refine these priors to give better predictions. The relative spatial layout of the human and the object involved in a HOI is greatly informative and should be utilized properly for predicting the interaction.

Existing work on HOI detection has not significantly leveraged this insight. Relative spatial locations are usually not given sufficient attention. Current approaches either use a small hand-created feature [12] or binary maps called interaction patterns (IPs) [3]. Using hand-created features has the potential downside

*Denotes equal contribution.

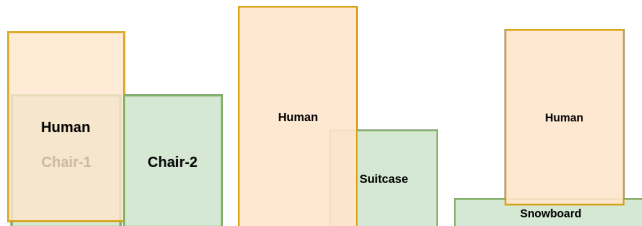


Fig. 1: The relative spatial relationship between a human and an object provides much information about their interaction. We can infer that in the left image, the human is probably **sitting** on Chair-1 and **not interacting** with Chair-2. In the middle, the human might be **dragging** the suitcase. And the person on the right is probably **riding** a snowboard.

of not being able to encode the fine-grained spatial relationships between objects. This limitation can be overcome by using interaction patterns, which are binary maps representing the locations of the human and the object in a HOI. Binary masks for the human and the object, as shown in figure 1 can be useful for predicting a prior on the interaction. This can be refined by using more visual information from the image.

We build on this idea for HOI detection. We address the question: how can we utilize the spatial locations of the entities to improve HOI detection? Our proposed approach consists of a layout branch and a visual branch. The layout module outputs a prediction which is used as a prior by the visual module. This prior prediction primes the visual branch which then outputs the final predictions. Priming the visual module using predictions from the layout module enables our model to fully utilize the spatial layout of the human and the object. We treat the relative geometry of these entities as high-quality cues.

Our layout and visual modules share information at multiple stages. Such information sharing between different modalities [7] and at different levels of a network [18,28] has been shown to make the models learn better representations. Lateral connections provide a way to share information between modules processing different types of information. For example, [7] proposed lateral connections between motion and appearance branches for video action recognition. Our layout module receives information from the visual branch through lateral connections in the model. This sharing of information enables the layout module to make stronger predictions about the predicate. We put the proposed approach in context of prior work in section 3.

We evaluate our proposed approaches on the challenging HICO-Det dataset [3]. In section 4, we first present results for a simple baseline algorithm which uses a good object detector and already achieves state-of-the-art results for HOI detection. Our proposed model reaches a mean average precision (mAP) of 24.79% on the HICO-Det dataset, which is about 2.8 absolute points higher than current state-of-the-art. We also conduct extensive analysis of our proposed method to tease out the reasons for these improvements.

Finally, we discuss some avenues for future research in section 5.

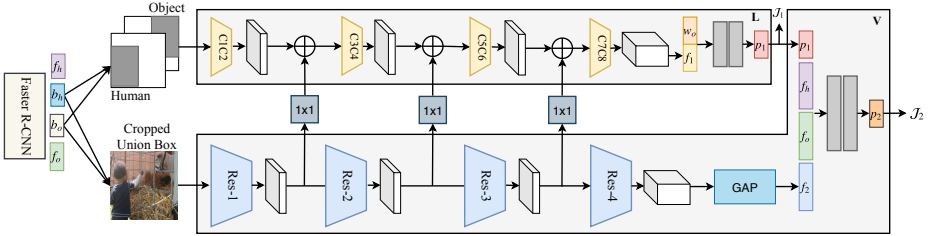


Fig. 2: Proposed Pipeline. A Faster R-CNN object detector is used to detect humans and objects in an image. For each human-object pair, the interaction pattern, and union box are input to L and V respectively. The predictions from L are used for priming V . The visual module, V takes the union box, predictions from L , RoI pooled human and object features from the object detector and outputs the final probabilities over the predicates.

The most important contributions of this paper are two fold: (1) propose spatial priming as a way to incorporate spatial layout of the human and object for HOI detection; (2) propose a model for HOI detection based on spatial priming and information sharing between a layout and a visual module. In addition, we conduct extensive analysis and evaluation of the proposed model to isolate sources of performance improvement and report state-of-the-art results.

2 Approach

The proposed model is composed of a relative layout module (L) and a visual module (V) which share information at multiple stages. The predictions from L are used to prime V and the final prediction is the output of V . Figure 2 shows the entire pipeline of our approach. Our model takes detections from an object detector in the form of human-object pairs as input and outputs the probabilities for the predicates. We describe each component of our model next.

2.1 Object Detector

We start by using Faster R-CNN [25] to detect all humans and objects in an image and create all candidate human-object pairs. Each pair has an associated human bounding box and an object bounding box, giving a union box (the smallest bounding box covering both the human and the object boxes). We crop the union box from the image and use it as an input to the visual module V .

We generate binary spatial maps (interaction patterns) of the same dimensions as the union box for the human and the object and stack these maps to produce a two-channel representation as shown in figure 2. These spatial maps are used as inputs to the layout module L .

2.2 Layout Module

The spatial layout network, L is based on the idea that the relative layout and the semantic category of the object can provide sufficient cues to determine the prior probabilities for the interaction between a human and an object (see discussion in section 1). We use a shallow CNN as the layout network. This network takes the stacked spatial maps as input. We add features from the visual module (described next) to intermediate layers in L via 1×1 convolutions. This provides visual context about the human and the object. After the final convolution layer, we apply global average pooling to get the layout feature f_1 .

Semantic knowledge. Only the relative spatial layout might not be enough to correctly determine the type of interaction. For example, in figure 1, it becomes difficult to predict the relationship without the object identity. Therefore, we incorporate the object identity in L . To include semantic information about the object, we concatenate f_1 with the `word2vec` [22] representation of the object, w_o and pass the concatenated vector through two fully-connected layers which give the probabilities over all predicates. Using semantic information about the object also helps in improving generalization of the model to interactions involving previously unseen objects (zero-shot detection). Using `word2vec` representations of the objects implicitly encodes semantic similarities between objects.

The output of the layout module are logits over the predicates which are used as an input to the visual module. These logits act as a prior to the visual module which refines its output based on this spatial prior.

2.3 Visual Module

The visual module V uses the predictions from L along with the visual information from the cropped union bounding box to make the final prediction. We use a deeper network as the base network in V . As mentioned above, intermediate features from V are added to L to provide appearance and contextual information to the layout module. The base network in V provides a feature vector f_2 after global average pooling the feature from the last convolution layer. We have two fully-connected layers at the end of the base convolution layers in V . As input to these layers, we concatenate the features f_2 , the prior predictions from the layout module p_1 , and the RoI-pooled human and object appearance features from the object detector, f_h and f_o . RoI-pooled features from the object detector provide explicit appearance information about the human and the object. The output of the visual module is the final output of the model.

2.4 Lateral Connections

We add features from intermediate layers in the visual module to intermediate layers in the layout module via 1×1 convolution layers. Adding the visual features to features in the layout module enables the model to explicitly share visual context not available in layout module. Therefore, L can benefit from the appearance of the two interacting entities along with their layout. This leads to a

stronger spatial prior for the final stages of the visual module. We will empirically demonstrate the importance of using this layout information in section 4.

2.5 Spatial Priming

Predictions from L based on the relative spatial layout prime the visual module. The layout module L provides strong priors for the predicate which are refined by the visual module which uses even more information about the human, object, and context appearance. Such priming enables the visual module to gain from the information contained in the relative spatial layout of the human and the object which is encoded by the binary spatial maps.

2.6 Training

We train L and V jointly. For both modules, we consider all predicates as independent and use a weighted binary-cross entropy loss. The weights are simply inversely proportional to the number of instances of the predicate in the dataset. The total loss is the sum of the two losses from L and V.

Note that, we predict the probabilities/confidence scores of each predicate for a human-object pair and not for the triplet `<human,predicate,object>` directly. This gives our method the ability to detect previously unseen HOI categories (zero-shot detection). To clarify, since we already have the object labels from the object detector, we only need to output the predicate in order to determine the interaction triplet. For example, the HICO-Det dataset contains 600 annotated HOI triplet categories of the form `<human,predicate,object>` but 117 predicates. In total, there are 9360 (117×80) possible interactions for this dataset. Only 600 of these are labeled. There might be more types of possible interactions than these. Our methods can potentially detect such unlabeled HOI categories too (table 3).

3 Related Works

Human-object interaction (HOI) prediction being a special and important subset of visual relationship prediction [20] is a well-studied problem. Early methods [10,35,34,36,5] for HOI prediction had mainly focused on developing hand-designed features and models. In particular, Yao *et al.* [35] proposed a random field model which encodes the idea that humans poses and objects can provide mutual context for each other. Delaitre *et al.* [4] built HOI features from spatial co-occurrences of body parts and objects. Hu *et al.* [14] used exemplars in the form of density functions representing an HOI. All of these are somewhat related to the proposed method owing to the use of the relative layout of humans and objects to reason about HOIs.

More recently, Mallya *et al.* [21] used CNN features from local and global context of a person along with a weighted loss to handle unbalanced training data. HO-RCNN [3] and InteractNet [9] employed separate human, object, and

interaction streams for HOI prediction. In particular, [9] jointly learned human and object detectors along with HOI detectors. However, these methods did not leave any scope for zero-shot HOI prediction. In [32], Xu *et al.* utilized gaze and pose information through a gaze-driven context-aware branch. Other methods [12,37,29] also used human-pose as fine-grained visual layout information. However, these methods require an additional model for predicting the pose. Unlike these, we argue that coarse relative layout along with the object identity provides sufficient cues to form a prior for interaction. We avoid the additional burden and potential errors of using a pose estimation model.

Several methods have utilized external **semantic knowledge for HOI prediction** [15,23,1]. In this work, we too have used semantic information in the form of word vectors for object classes. These help in transferring knowledge from an object to other similar object classes. Using semantic knowledge also helps in generalizing to zero-shot HOI categories. Zero-shot HOI detection has previously been studied in [1,26]. This followed several works on zero-shot object recognition [31,16] and zero-shot object detection [2].

Like the proposed model, Li *et al.* [17] had also used priors for refining predictions. However, they learned “interactiveness priors” which only inform whether a human and an object are interacting or not. We, instead, add a prior which informs about the HOI category based on the relative spatial layout.

Relative spatial layout is an important cue for predicting their interaction. Some prior works have tried to incorporate the spatial relationship by encoding it as a small hand-designed feature and passing it as input to a neural network [12,1]. Chao *et al.* [3] proposed “interaction patterns” for encoding the relative spatial location. Gao *et al.* [8] also used such interaction patterns as a secondary branch of the model. However, it can be argued that even these methods considered relative layout as secondary information to the visual features. In this paper, we use IPs as binary spatial maps to represent the relative layout of the human and the object. We present a principled approach for exploiting the information contained in such spatial maps. Our model uses a small CNN to combine visual, semantic, and geometric information to make a prediction for the predicate. This prediction is used as a prior for our final visual appearance-based branch.

Lateral connections have been used for merging information from different spatial resolutions [18], for fusing optical and visual streams in two-stream networks [7], and for fusing coarse and fine temporal resolutions [6]. Shrivastava *et al.* [27] also used such lateral connections for priming an object detector by contextual information from semantic segmentation. Feature Pyramid Network (FPN) [18] used lateral connections for building high-level semantic feature maps for object detection. Similarly, in [28] bottom-up and top-down pathways for object detection are connected using lateral connections.

4 Experiments

We start with a brief description of the dataset and evaluation metrics and provide implementation details for our approach. We then discuss the model

performance in fully-supervised and zero-shot settings. Finally, we discuss and analyze the model through extensive ablation studies.

4.1 Dataset and evaluation metrics

Following prior work, we use the challenging HICO-Det dataset [3] for evaluating our approach. This dataset contains 600 HOI triplet $\langle \text{human}, \text{predicate}, \text{object} \rangle$ categories involving 117 predicates and 80 objects. These categories are divided into: (a) Rare - 138 categories with less than 10 training samples, and (b) Non-rare categories. There are about 38,000 training images containing about 120,000 interactions and about 9,600 test images with about 33,400 HOIs.

Mean average precision (mAP) is used as the evaluation metric. A detected triplet is considered correct if both human and object overlaps (IoU) with the ground truth are greater than 0.5. Performance is reported for the full set of 600 classes and also for the rare and non-rare classes separately.

Due to its inconsequential size ($< 6,000$ training images and just 26 predicates), the V-COCO dataset [11] does not provide any new insights into HOI detection approaches. Unsurprisingly, most recent state-of-the-art methods [1,12,23] do not use V-COCO. To save space for an exhaustive analysis of our model, we discuss V-COCO in the supplementary material.

4.2 Implementation Details

Following the state-of-the-art [1], we start by fine-tuning a ResNet-101 [13] based Faster R-CNN [25] object detector for the HICO-Det dataset [3]. The detector was originally trained on the COCO dataset [19] which has the same 80 object classes. Fine-tuning enables the detector to confidently detect objects more likely to be involved in an interaction. This helps in improving the performance of downstream predicate classifiers. Please see supplementary materials for details.

To create the training dataset, we consider all detections for which the detection confidence is greater than 0.75 and the overlap with a ground-truth human or object box is greater than 0.7. We create human-object pairs for each image using these detections and end up with about 250,000 training HOI triplets. For test proposals, we select only those object and human proposals which have a confidence score greater than 0.9 for a particular class. This ensures that we get only high confidence object detections and make fewer errors because of incorrectly detected objects and humans. Each detection has an associated feature vector and bounding boxes. We use the human and object bounding boxes, b_h and b_o respectively to compute the union box and the binary spatial maps.

For our model, the visual module is a ResNet-50 network and the layout module is a shallow 8-layer CNN (see supplementary material for details). Each layer of L contains a ReLU non-linearity and batch-normalization. We add lateral connections from each Residual block in V to L , i.e., there are three lateral connections. Features from the residual blocks, Res-1, Res-2, and Res-3 are added to the respective places in L as shown in figure 2. The fully connected layers are of sizes 1024 and 512 in both L and V . We reiterate that both L and V give the

Table 1: Baseline results (mAP %)

Method	Full (600 classes)	Rare (138 classes)	Non-rare (462 classes)
Baseline ResNet-50	20.80	15.63	22.34
Baseline ResNet-50+ f_h + f_o	21.49	14.43	23.60

probabilities for the 117 predicates. This is unlike many previous methods which directly predict the HOI triplets (600 categories). We use the object labels from the object detector to output the final triplet. This also enables us to detect previously unseen HOIs (zero-shot detection).

In all our experiments, we train the model for 10 epochs with an initial learning rate of 0.1 which is dropped by a tenth every 3 epochs. Note that the object detector and the semantic word-vectors are frozen while training our models, i.e., the detector needs to be trained only once.

4.3 Results

Strong Baseline. We start with a baseline CNN which predicts the predicates just based on the cropped union box. We first use a ResNet-50 (R-50) network as the classifier which takes a cropped union box as input and outputs the probabilities for each predicate. This network achieves an mAP of 20.80% for the HICO-Det test set. This is a strong albeit simple baseline which is already better than the current state-of-the-art performance of 19.40% (table 2). This reveals that the existing methods can benefit from simplifying the algorithm and just using a better object detector and a stronger feature extractor. A simple model like classifying the union box obtained from detections from an object detector is enough to achieve better performance than existing methods. Adopting the common practice [17,9] of using the features from the object detector, we append the RoI-pooled features to the features from the R-50, and obtain an mAP of 21.49%. We summarize these results in table 1.

Comparison with Prior Work. We compare the performance of our model with past work in table 2. Our model achieves an mAP of 24.79%, which is over 2.8 absolute percentage points higher than the current state-of-the-art method [1] on the Full set of the HICO-Det dataset. Our method also performs about 4.2 absolute percentage points better on Non-rare classes. Interestingly, at the same time, even though we do not target them explicitly, our model achieves competitive performance on Rare classes too. Note that the methods in [1] and [23] are explicitly designed to target rare and unseen classes.

We also point out that, even using the original COCO detector instead of our fine-tuned detector, our model achieves an mAP of 19.45%. This is the highest among all methods using an object detector trained on COCO. In particular, the mAP achieved by the proposed method is significantly higher (2 – 12% mAP) than previous methods [3,8,30] which aim to utilize the relative spatial layout of the two entities. In addition, we obtain a higher performance than RPNN [37]

Table 2: Comparison with prior work. The performance (mAP %) obtained by our method is significantly higher than existing methods.

Method	Full (600 classes)	Rare (138 classes)	Non-rare (462 classes)
Shen <i>et al.</i> [26]	6.46	4.24	7.12
HO-RCNN + IP [3]	7.30	4.68	8.08
HO-RCNN + IP + S [3]	7.81	5.37	8.54
InteractNet [9]	9.94	7.16	10.77
GPNN [24]	13.11	9.34	14.23
iHOI [32]	13.39	9.51	14.55
Xu <i>et al.</i> [33]	14.70	13.26	15.13
ICAN [8]	14.84	10.45	16.15
Wang <i>et al.</i> [30]	16.24	11.16	17.75
Gupta <i>et al.</i> [12]	17.18	12.17	18.68
Interactiveness Prior [17]	17.22	13.51	18.32
RPNN [37]	17.35	12.78	18.71
PMFNet [29]	17.46	15.65	18.00
Peyre <i>et al.</i> [23]	19.40	15.40	20.75
Functional Gen. [1]	21.96	16.43	23.62
Ours	24.79	14.77	27.79

and PMFNet [29] which use additional pose information using models trained on large datasets. This demonstrates the strength of Spatial Priming as a way of modeling the geometric layout.

Table 3: Zero-shot HOI detection (mAP %).

Method	Unseen (120 classes)	Seen (480 classes)	All (600 classes)
Shen <i>et al.</i> [26]	5.62	-	6.26
Functional Gen. [1]	10.93	12.60	12.26
Ours	11.06	21.41	19.34

Zero-Shot HOI Detection. The proposed approach can help improve the performance for zero-shot HOI detection. Table 3 compares the performance of our method with the state-of-the-art methods [26,1] on zero-shot HOI detection. Prior work divides the classes into a set of 120 unseen and 480 seen classes. We use the same setting here. The model is trained with training data for only the seen classes and is evaluated on the set of unseen classes. Note that the classes are divided such that there is at least one interaction involving each of the 80 objects in the training set, i.e., the model is trained with at least one HOI involving each object. From table 3 we observe that our model achieves a higher mAP than [1] for Unseen classes while also improving the mAP for Seen classes by a huge margin. We have used the same train-test splits as [1].

Table 4: Ablation studies for the model. We report mAP (%) in each case. In all sub-tables “Standard” refers to the model shown in figure 2.

(a) **Effect of w_o .** Row 2 is the standard model without w_o . Note that the performance without w_o is lower than the Standard case. This is particularly true for the Rare classes.

Setting	Full	Rare	Non-rare
Standard	24.79	14.77	27.79
Standard - w_o	24.47	12.16	28.14

(b) **Lateral connection methods.** Concat is the model with lateral additions replaced by concatenation. 3x3add uses 3×3 convs in lateral connections instead of 1×1 used in the Standard setting.

Setting	Full	Rare	Non-rare
Standard	24.79	14.77	27.79
Concat	24.00	13.91	27.02
3x3add	24.21	13.34	27.47

(c) **Importance of L.** ImgCNNA-ImgR50 is the model where input to L is the cropped union box. Similarly, in ImgR50-ImgR50, the layout module is a ResNet-50 with the union box as input. (Standard is IPCNNA-ImgR50)

Setting	Full	Rare	Non-rare
Standard	24.79	14.77	27.79
ImgCNNA-ImgR50	22.28	10.87	25.69
ImgR50-ImgR50	24.07	11.96	27.68

(d) **Utility of f_h, f_o .** Concat contains concatenated lateral connections. Standard- f_h-f_o has no f_h and f_o . Standard-Larger contains larger hidden layers and no f_h and f_o . Similarly for Concat- f_h-f_o and Concat-Larger.

Setting	Full	Rare	Non-rare
Standard	24.79	14.77	27.79
Standard- f_h-f_o	22.32	13.14	25.07
Standard-Larger	24.60	13.58	27.89
Concat	24.00	13.91	27.02
Concat- f_h-f_o	21.87	13.05	24.51
Concat-Larger	23.41	14.44	26.09

(e) **Different lateral connections.** Conn1 is the model with just one lateral connection from V to L which is at Res-1. Conn2 has just one lateral connection at Res-2 and Conn3 has the lateral connection at Res-3. L-V has all connections from L to V.

Setting	Full	Rare	Non-rare
Standard	24.79	14.77	27.79
L-V	23.81	13.44	26.91
Conn1	23.63	10.75	27.48
Conn2	24.01	12.86	27.34
Conn3	22.87	11.42	26.28

4.4 Ablation Analysis

We now extensively analyze our model in tables 4, 5, and 6.

Importance of w_o . Word-vectors w_o encode the semantic similarities between objects. Table 4a shows that using the word-vector in the layout module leads to performance improvement. The complete model which uses the `word2vec` vectors w_o achieves an mAP 24.79%. Removing this word-vector leads to a lower performance (24.47%).

Type of Lateral Connection. Table 4b illustrates that adding the features from the visual module to the geometric module achieves higher performance than concatenating the features. The mAP in the case of addition of features is 24.79%. Compare this to the mAP of 24% when the features are concatenated instead. The reason for this is that adding features from the visual module forces L to explicitly focus on the human and object. This ensures that the relevant regions of the image are given more importance. Similarly, when using 3×3 convolutions in the lateral connections instead of 1×1 , the performance is slightly

lower. This is because using 3×3 convolutions increase the receptive field of the features. This dilutes the focus on the human and the object which in turn leads to a lower performance.

Layout Module. The importance of using the relative spatial layout of the human and object is demonstrated using the data in table 4c. The first row in the table is the standard case when the human and object spatial maps are given as input to the shallow layout network. This model gives an mAP of 24.79%. Now, if we remove the binary spatial maps (IP) and input the cropped union box image to the layout module too, the performance of the model drops to just 22.28% (second row). Note that this model has the same number of parameters as the previous model. The only difference is the input to L. To ensure that the drop in performance is not due to a weak layout network, we replace the small CNN in the layout module with a ResNet-50 network. Again, the input to both the layout and visual branches is the cropped union box. Even this model, with a much larger number of parameters than the standard case, gives an mAP of just 24.07%. This shows that relative spatial layout of the human and the object provides irreplaceable information for determining the type of interaction.

Importance of f_h and f_o . From table 4d, we observe that a model gives a lower performance if appearance features from the object detector are not used. For example, the Standard model reaches an mAP of 24.79% while the Standard model trained without f_h and f_o reaches only 22.32%. Similarly, the performance for the Concat model (from table 4b) goes down from 24% to just 21.87% on removing the features. Clearly, f_h , and f_o help in achieving higher performance. Recall that we had observed the same effect with the Baseline model (table 1).

To analyze if these improvements are because of a larger number of parameters, we removed f_h and f_o and increase the sizes of the fully connected layers such that the number of trainable parameters in this model and the Standard model are roughly the same. We call this model Standard-Larger. This model gives an mAP of 24.60%. This is down from 24.79% obtained by the Standard model. Similarly, the Concat-Larger model gives an mAP of 23.41%, down from the Concat model which gave 24%. So, even though some of the performance gain when using the appearance features could be due to a larger number of parameters, it does not explain the whole difference. We believe that the features f_h and f_o do, in fact, provide useful information for predicting the HOI.

Different Connections. We show that having lateral connections at multiple depths in the network is important for obtaining a good performance. We study whether having just one lateral connection can be enough. From table 4e, we infer that the answer is *no*. Just one lateral connection after either Res-1 block, Res-2 block, and Res-3 block (rows 3, 4, and 5 respectively) gives worse performance than having connections at all three places. In particular, having just one connection after Res-3 gives the lowest performance. This is because by this depth the visual module loses most spatial information and the layout module does not benefit from adding visual features. This shows that frequent information sharing between the two modules via lateral connections gives significant perfor-

mance improvements. We also observe that passing information from the spatial layout module to the visual module also achieves a lower mAP.

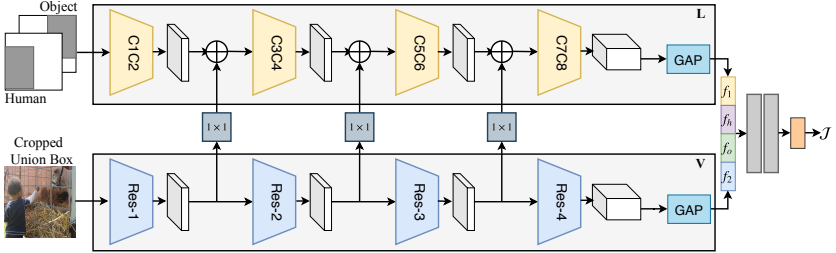


Fig. 3: **No priming (NP)**. This model removes the spatial priming from our model (figure 2). Human and object bounding boxes from an object detector give the interaction patterns and the union box. Global Average Pooled (GAP) features from the geometry and visual networks are concatenated to the human and object RoI pooled features from the object detector. Two FC layers are used to get the probabilities/confidences over the predicates.

To analyze the effect of each of the component in our model in more detail, we conduct ablation studies in two further settings. First, we study the utility and behaviour of lateral connections without priming. We remove the loss \mathcal{J}_1 and instead of adding layout priors, p_1 to the visual module, we directly add the global average pooled features, f_1 . This gives the model shown in figure 3. We call this model NP.

No Priming. The first row in table 5 gives the performance of the NP model (no priming) shown in figure 3. This model achieves an mAP of 23.41% on the Full HICO-Det dataset. Notice that this is higher than the Baseline model discussed earlier (21.49% table 1). This highlights the importance of the spatial layout even in this simpler setting.

Table 5: **NP Results** (mAP %). NP is the model shown in figure 3 with lateral connections from V to L. NC is the same model without lateral connections. Similarly, L-V has connections from the layout branch to the visual branch. V-L-concat concatenates the features from V and L instead of adding.

Method	Full (600 classes)	Rare (138 classes)	Non-rare (462 classes)
V-L-add (NP)	23.41	12.14	26.78
NC	22.56	12.78	25.48
L-V	22.45	12.23	25.50
V-L-concat	22.76	11.78	26.04

We further analyze the behavior of this model in different conditions. In table 5 V-L is the model with lateral connections from the visual module (V) to the layout module (L). To illustrate the positive impact of these lateral connections, we remove all lateral connections and train the resulting model. This model is called “NC” (no connection) in table 5. NC reaches an mAP of only 22.56%. Clearly, lateral connections enable better utilization of the relative spatial layout of a person and an object. However, note that this is still higher than the Baseline model (21.49%), clearly demonstrating that leveraging layout information is important for improving HOI detection performance.

Further, we observe that connections from layout module to the visual module (L-V) give almost the same performance as having no connection (NC). Also, the final row in table 5 is the case where we concatenate the intermediate features from the visual module to the features of the layout module instead of adding. This model, though better than having no connections, is still worse than the V-L model. We believe that in the case of concatenation, the network does not learn to attend to the human and the object. On the other hand, when we add the features instead, we explicitly force the network to attend to the human and object regions of the image. This enables it to learn better mappings from human and object appearances to the correct predicate. Recall that we had seen similar behavior in table 4b.

Next, we study the effect of removing lateral connections from our model. This is an important case and will show how informative the layout module is on its own. This will help us pinpoint how the components of our model behave in the presence of only spatial priming without lateral connections. We remove the lateral connections from our model in figure 2. This gives us the model shown in figure 4. We call this model NL.

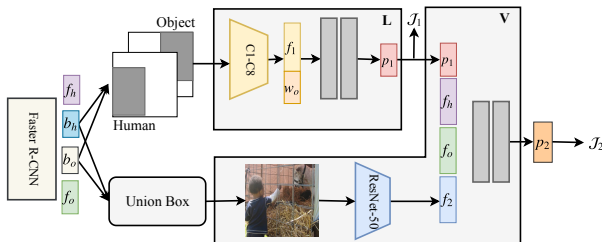


Fig. 4: **No lateral connections (NL)**. We remove lateral connections from our model (figure 2). Now, L predicts the interaction just based on the spatial layout. These predictions are given as a prior to V which also uses the union bounding box and the RoI pooled features from the object detector to make the final prediction.

No Lateral Connections. Results and ablation studies for the NL model are listed in table 6. The best model reaches 23.90% in mAP on the HICO-Det dataset. It contains a shallow layout branch L which predicts the predicate based only on the spatial layout of the human and the object. This prediction is used

as a prior by the visual network V which gives the final prediction. We highlight the performance of the layout network L . It achieves an mAP of 18.35% on the Full set of HICO-Det. This shows that there is significant information about the interaction category contained in the relative spatial layout of the human and object. When properly trained, using only this information might be better than most existing methods (13/15 methods in table 2).

Again, the importance of a layout-based prior is apparent when comparing the performance of this model with the performance of the baseline R-50 model which had reached only 21.49% (table 1). The last row in table 6 shows that removing the word vector w_o from the model leads to a drop in performance. This is driven down by the reduction in the performance of the layout model L which went from 18.35% in the usual case to just 16.33%. Removing the appearance features from the detector, f_h and f_o , also results in lower performance. We had seen the same trends even in the presence of lateral connections in table 4. Also, note that the performance for NL (23.90%) is higher than the performance for NP (23.41% table 5), showing that the idea of spatial priming is a significant source of improvement achieved by our proposed model.

Table 6: **NL Results** (mAP %). First row (NL) is the model shown in figure 4. NL - f_h - f_o represents the model trained without the appearance features from the object detector. NL - w_o is NL without the word vector for the object.

Method	Model	Full (600 classes)	Rare (138 classes)	Non-rare (462 classes)
NL	L	18.35	8.20	21.38
	V	23.90	10.82	27.81
NL - f_h - f_o	L	17.44	10.14	19.62
	V	23.19	14.71	25.72
NL - w_o	L	16.33	8.45	18.69
	V	22.91	11.29	26.39

5 Discussion and Conclusion

We discuss some avenues for further improvements and finally conclude.

5.1 Discussion

In this paper, we have not explicitly considered ways of improving detection for rare classes. The competitive performance for rare classes in table 2 is a by-product of our approach, particularly, using semantic knowledge in the form of `word2vec` representations. HOI datasets will always suffer from the long-tail problem. Future research should focus on improving performance for rare classes. Clever class-weighting strategies and using more semantic knowledge as in [23] could be some ways of going forward.

Another limitation of our method is the dependence on a pre-trained object detector. Future work should also focus on jointly training the HOI prediction

model and the object detector. Since HOI detection and object detection have complementary objectives (a better object detector leads to better HOI detection), this line of approach could significantly improve performance for both HOI detection and object detection.

5.2 Conclusion

We have presented an approach for using the relative layout information of a human and an object for detecting interactions between them. Our proposed model consists of two modules: one for processing the relative spatial layout of a human and an object, and the other for processing visual information. The visual module is primed using the prediction of the layout module. We have systematically analyzed the model and our experiments shown that this method can significantly out-perform state-of-the-art methods for HOI detection.

Acknowledgement

This project was supported by the Intelligence Advanced Research Projects Activity (IARPA) via Department of Interior/Interior Business Center (DOI/IBC) contract number D17PC00345 and by DARPA via ARO contract number W911NF2020009. The U.S. Government is authorized to reproduce and distribute reprints for Governmental purposes not withstanding any copyright annotation thereon.

Disclaimer: The views and conclusions contained herein are those of the authors and should not be interpreted as necessarily representing the official policies or endorsements, either expressed or implied of IARPA, DOI/IBC, DARPA, ARO, or the U.S. Government.

S1 Architecture of Layout Module

The layout module is a shallow 8-layer CNN. Each layer of L contains a ReLU non-linearity and batch-normalization. See details of the convolution layers in table S1. We add lateral connections from each Residual block in V to L, i.e., there are three lateral connections. Features from the residual blocks, Res-1, Res-2, and Res-3 are added to the respective places in L.

Table S1: **Architecture of L.** C1-C8 are convolution layers. Layer dimensions are in the shape `kernel_width × kernel_height × output_channels`. Numbers in parenthesis are strides.

Layer	Layer Dimensions	Output Sizes
C1C2	7×7×64 (2), MaxPool (2), 3×3×256 (1)	56×56×256
C3C4	1×1×128 (1), 3×3×512 (2)	28×28×512
C5C6	1×1×256 (1), 3×3×1024 (2)	14×14×1024
C7C8	1×1×512 (1), 3×3×2048 (2)	7×7×2048
GAP	7×7	1×1×2048
FC1	1024	1024
FC2	512	512

S2 V-COCO

Similar to prior methods [9,37,29] we use the 24 action classes involving a person and an object. We use our ResNet-101 object detector to extract the human and object bounding boxes from each image. For generating the training set, we use all proposals which overlap with a ground-truth entity box with an IoU greater than 0.5. For testing, we use human and object proposals with confidence > 0.8. A major difference between the HICO-Det dataset [3] and V-COCO is the absence of annotations for the **no-interaction** or **background** class. We generate samples for **no-interaction** by considering un-labeled human-object interactions as belonging to this class. Following the standard practice in object detection [25], we use the background and labeled classes in a ratio of 3:1.

Table S2 shows that the performance achieved by Spatial Priming (49.2% mAP) is significantly higher than most existing methods. In table S3, we list the class-wise AP obtained by our method for the 24 classes under consideration.

S3 Analysis of Object Detector

In this section, we analyze how fine-tuning the object detector on the HICO-Det dataset helps in improving the HOI detection performance for HICO-Det. Figure S1 shows the detections on test images of HICO-det for a ResNet-101 Faster R-CNN trained on COCO (top) and HICO (bottom). For every object

Table S2: Comparison with prior work for the V-COCO dataset. The performance (mAP_{role} %) obtained by our method is higher than existing methods.

Method	mAP_{role}
Gupta et al. [11]	31.8
InteractNet [9]	40.0
GPNN [24]	44.0
ICAN [8]	45.3
RPNN [37]	47.5
Wan et al. [29]	48.6
RP _{T2} CD [17]	48.7
Spatial Priming (Ours)	49.2

Table S3: Class-wise AP obtained by our Spatial Priming approach for the V-COCO dataset.

Class	AP_{role}
hold-obj	36.81
sit-instr	32.94
ride-instr	64.34
look-obj	42.34
hit-instr	69.02
hit-obj	39.39
eat-obj	46.70
eat-instr	13.31
jump-instr	52.69
lay-instr	31.66
talk_on_phone-instr	30.15
carry-obj	37.45
throw-obj	41.72
catch-obj	52.94
cut-instr	34.04
cut-obj	48.30
work_on_computer-instr	64.85
ski-instr	46.03
surf-instr	76.43
skateboard-instr	86.68
drink-instr	45.01
kick-obj	78.37
read-obj	33.18
snowboard-inst	75.36
Average Role AP	49.15

class in HICO-det, we select all boxes with confidence score greater than 0.9 and apply Non-maximum Supression (NMS) with an IoU threshold of 0.5 for visualizing the results. The ground truth boxes are marked in green and the detector outputs are marked in red.

We observe that annotations of COCO dataset are very tight around the object unlike the HICO-det dataset. While a detector trained on COCO gives us tight boxes around the object, it can often be detrimental when evaluated on boxes which are not as tight. In the HICO-det dataset, most of the objects in the background have not been labeled because the objects are usually not part of an interaction, or are out of focus. While detectors trained on COCO densely detect objects in the image, that can be detrimental for the task of HOI detection on HICO-Det. By densely detecting all the objects in the image, we increase the number of HOI proposals which in turn results in a large number of false positives. Using a detector trained for object detection (e.g. COCO) directly for the task of HOI detection can often lead to inferior results.

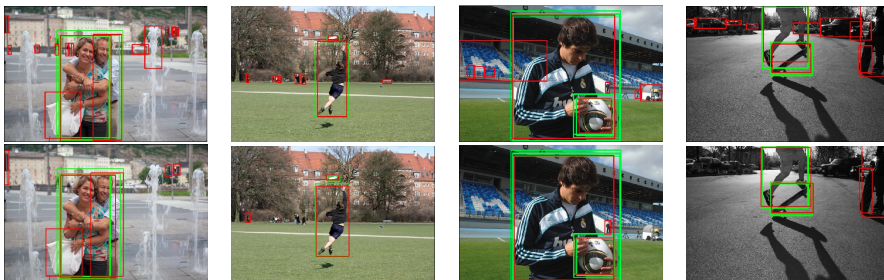


Fig. S1: Qualitative Analysis: Comparison of the proposals from (top) a detector trained on COCO and (bottom) a detector fine-tuned on objects in HICO-Det. The images shown are from the test set of HICO-Det. The green boxes are the ground truth annotations and red boxes are the detection outputs. NMS with a threshold of 0.5 was applied on the proposals. Detectors fine-tuned on HICO give fewer false positives.

References

1. Bansal, A., Rambhatla, S.S., Shrivastava, A., Chellappa, R.: Detecting human-object interactions via functional generalization. arXiv preprint arXiv:1904.03181 (2019) [6](#), [7](#), [8](#), [9](#)
2. Bansal, A., Sikka, K., Sharma, G., Chellappa, R., Divakaran, A.: Zero-shot object detection. In: The European Conference on Computer Vision (ECCV) (September 2018) [6](#)
3. Chao, Y.W., Liu, Y., Liu, X., Zeng, H., Deng, J.: Learning to detect human-object interactions. arXiv preprint arXiv:1702.05448 (2017) [1](#), [2](#), [5](#), [6](#), [7](#), [8](#), [9](#), [16](#)
4. Delaitre, V., Sivic, J., Laptev, I.: Learning person-object interactions for action recognition in still images. In: Advances in neural information processing systems. pp. 1503–1511 (2011) [5](#)
5. Desai, C., Ramanan, D.: Detecting actions, poses, and objects with relational phraselets. In: European Conference on Computer Vision. pp. 158–172. Springer (2012) [5](#)
6. Feichtenhofer, C., Fan, H., Malik, J., He, K.: Slowfast networks for video recognition. arXiv preprint arXiv:1812.03982 (2018) [6](#)
7. Feichtenhofer, C., Pinz, A., Wildes, R.: Spatiotemporal residual networks for video action recognition. In: Advances in neural information processing systems. pp. 3468–3476 (2016) [2](#), [6](#)
8. Gao, C., Zou, Y., Huang, J.B.: ican: Instance-centric attention network for human-object interaction detection. arXiv preprint arXiv:1808.10437 (2018) [6](#), [8](#), [9](#), [17](#)
9. Gkioxari, G., Girshick, R., Dollár, P., He, K.: Detecting and recognizing human-object interactions. arXiv preprint arXiv:1704.07333 (2017) [5](#), [6](#), [8](#), [9](#), [16](#), [17](#)
10. Gupta, A., Davis, L.S.: Objects in action: An approach for combining action understanding and object perception. In: Computer Vision and Pattern Recognition, 2007. CVPR'07. IEEE Conference on. pp. 1–8. IEEE (2007) [5](#)
11. Gupta, S., Malik, J.: Visual semantic role labeling. arXiv preprint arXiv:1505.04474 (2015) [7](#), [17](#)
12. Gupta, T., Schwing, A., Hoiem, D.: No-frills human-object interaction detection: Factorization, layout encodings, and training techniques. The IEEE International Conference on Computer Vision (ICCV) pp. 9677–9685 (October 2019) [1](#), [6](#), [7](#), [9](#)
13. He, K., Zhang, X., Ren, S., Sun, J.: Deep residual learning for image recognition. 2016 IEEE Conference on Computer Vision and Pattern Recognition (CVPR) pp. 770–778 (2016) [7](#)
14. Hu, J.F., Zheng, W.S., Lai, J., Gong, S., Xiang, T.: Recognising human-object interaction via exemplar based modelling. In: Proceedings of the IEEE International Conference on Computer Vision. pp. 3144–3151 (2013) [5](#)
15. Kato, K., Li, Y., Gupta, A.: Compositional learning for human object interaction. In: Proceedings of the European Conference on Computer Vision (ECCV). pp. 234–251 (2018) [6](#)
16. Kodirov, E., Xiang, T., Gong, S.: Semantic autoencoder for zero-shot learning. arXiv preprint arXiv:1704.08345 (2017) [6](#)
17. Li, Y.L., Zhou, S., Huang, X., Xu, L., Ma, Z., Fang, H.S., Wang, Y., Lu, C.: Transferable interactiveness knowledge for human-object interaction detection. The IEEE Conference on Computer Vision and Pattern Recognition (CVPR) (June 2019) [6](#), [8](#), [9](#), [17](#)
18. Lin, T.Y., Dollár, P., Girshick, R., He, K., Hariharan, B., Belongie, S.: Feature pyramid networks for object detection. In: Proceedings of the IEEE Conference on Computer Vision and Pattern Recognition. pp. 2117–2125 (2017) [2](#), [6](#)

19. Lin, T.Y., Maire, M., Belongie, S., Hays, J., Perona, P., Ramanan, D., Dollár, P., Zitnick, C.L.: Microsoft coco: Common objects in context. In: European conference on computer vision. pp. 740–755. Springer (2014) [7](#)
20. Lu, C., Krishna, R., Bernstein, M., Fei-Fei, L.: Visual relationship detection with language priors. In: European Conference on Computer Vision. pp. 852–869. Springer (2016) [5](#)
21. Mallya, A., Lazebnik, S.: Learning models for actions and person-object interactions with transfer to question answering. In: European Conference on Computer Vision. pp. 414–428. Springer (2016) [5](#)
22. Mikolov, T., Sutskever, I., Chen, K., Corrado, G.S., Dean, J.: Distributed representations of words and phrases and their compositionality. In: NIPS (2013) [4](#)
23. Peyre, J., Laptev, I., Schmid, C., Sivic, J.: Detecting unseen visual relations using analogies. The IEEE International Conference on Computer Vision (ICCV) (October 2019) [6](#), [7](#), [8](#), [9](#), [14](#)
24. Qi, S., Wang, W., Jia, B., Shen, J., Zhu, S.C.: Learning human-object interactions by graph parsing neural networks. arXiv preprint arXiv:1808.07962 (2018) [9](#), [17](#)
25. Ren, S., He, K., Girshick, R., Sun, J.: Faster r-cnn: Towards real-time object detection with region proposal networks. In: NIPS. pp. 91–99 (2015) [3](#), [7](#), [16](#)
26. Shen, L., Yeung, S., Hoffman, J., Mori, G., Fei-Fei, L.: Scaling human-object interaction recognition through zero-shot learning. In: 2018 IEEE Winter Conference on Applications of Computer Vision (WACV). pp. 1568–1576. IEEE (2018) [6](#), [9](#)
27. Shrivastava, A., Gupta, A.: Contextual priming and feedback for faster r-cnn. In: European Conference on Computer Vision. pp. 330–348. Springer (2016) [6](#)
28. Shrivastava, A., Sukthankar, R., Malik, J., Gupta, A.: Beyond skip connections: Top-down modulation for object detection. arXiv preprint arXiv:1612.06851 (2016) [2](#), [6](#)
29. Wan, B., Zhou, D., Liu, Y., Li, R., He, X.: Pose-aware multi-level feature network for human object interaction detection. In: The IEEE International Conference on Computer Vision (ICCV) (October 2019) [6](#), [9](#), [16](#), [17](#)
30. Wang, T., Anwer, R.M., Khan, M.H., Khan, F.S., Pang, Y., Shao, L., Laaksonen, J.: Deep contextual attention for human-object interaction detection. In: The IEEE International Conference on Computer Vision (ICCV) (October 2019) [8](#), [9](#)
31. Xian, Y., Schiele, B., Akata, Z.: Zero-shot learning-the good, the bad and the ugly. arXiv preprint arXiv:1703.04394 (2017) [6](#)
32. Xu, B., Li, J., Wong, Y., Kankanhalli, M.S., Zhao, Q.: Interact as you intend: Intention-driven human-object interaction detection. IEEE Transactions on Multimedia (2019) [6](#), [9](#)
33. Xu, B., Wong, Y., Li, J., Zhao, Q., Kankanhalli, M.S.: Learning to detect human-object interactions with knowledge. In: The IEEE Conference on Computer Vision and Pattern Recognition (CVPR) (June 2019) [9](#)
34. Yao, B., Fei-Fei, L.: Grouplet: A structured image representation for recognizing human and object interactions. In: Computer Vision and Pattern Recognition (CVPR), 2010 IEEE Conference on. pp. 9–16. IEEE (2010) [5](#)
35. Yao, B., Fei-Fei, L.: Modeling mutual context of object and human pose in human-object interaction activities. In: Computer Vision and Pattern Recognition (CVPR), 2010 IEEE Conference on. pp. 17–24. IEEE (2010) [5](#)
36. Yao, B., Jiang, X., Khosla, A., Lin, A.L., Guibas, L., Fei-Fei, L.: Human action recognition by learning bases of action attributes and parts. In: Computer Vision (ICCV), 2011 IEEE International Conference on. pp. 1331–1338. IEEE (2011) [5](#)

37. Zhou, P., Chi, M.: Relation parsing neural network for human-object interaction detection. In: The IEEE International Conference on Computer Vision (ICCV) (October 2019) [6](#), [8](#), [9](#), [16](#), [17](#)